Purdue University
Purdue e-Pubs

International Refrigeration and Air Conditioning Conference

School of Mechanical Engineering

2008

Simulation of the Effects of a Non-Adiabatic Capillary Tube on Refrigeration Cycle

Sanggoon Park
Pusan National University

Kidong Son
Pusan National University

Jihwan Jeong
Pusan National University

Lyunsu Kim
LG Electronics

Follow this and additional works at: http://docs.lib.purdue.edu/iracc

Simulation of the Effects of a Non-Adiabatic Capillary Tube on Refrigeration Cycle

Sang-Goo Park[1], Kidong Son[1], Ji Hwan Jeong[1†], Lyun-Su Kim[2]

[1]School of Mechanical Engineering, Pusan National University
Busan, South Korea

[2]LG Electronics, Engineering Design Department Refrigeration Division
Changwon, Gyeongnam, South Korea

[†]TEL : +82-51-510-3050 E-mail : jihwan@pusan.ac.kr

ABSTRACT

The simulation of refrigeration cycle is important since the experimental approach is too costly and time-consuming. The present simulation focuses on the effect of capillary tube-suction line heat exchangers (CT-SLHX), which are widely used in small vapor compression refrigeration systems. The simulation of steady states is based on fundamental conservation equations of mass and energy. These equations are solved simultaneously through iterative process. The non-adiabatic capillary tube model is based on homogeneous two-phase model. This model is used to understand the refrigerant flow behavior inside the non-adiabatic capillary tubes. The simulation results show that both of the location and length of heat exchange section influence the coefficient of performance (COP). These results can be used in either design calculation of capillary tube length for refrigeration cycle or effect of suction line heat exchanging on refrigeration cycle.

1. INTRODUCTION

Recent world-wide concern about global environments requires energy consuming systems to be more efficient. Small refrigeration system is not an exemption. Conventional domestic refrigerator and small capacity air-conditioner take advantage of capillary tube as an expansion device. The capillary tube highly generates entropy to perform its function. Suction line heat exchange in one of the ways that can recover the entropy generation of expansion device. However, it is still required to optimize the refrigeration cycle with suction-line heat exchanger. This optimization work can be carried out using experimental methods and analytic methods. Computer simulation must be one of the valuable means to reduce efforts and expense. The research about performance prediction of refrigeration cycles has been of interest since the late 70's. Hitler and Glicksman (1976), Fischer and Rice (1980), Domanski (1982) developed simulation programs to predict performance of a steady state heat pump.
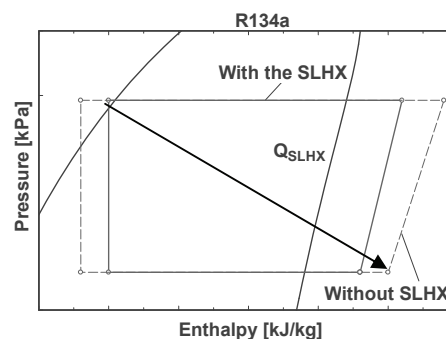

Figure 1: Mollier diagram for a refrigeration cycle with (solid line) and without (dashed line) SLHX

The SLHX (Suction Line Heat eXchanger) is used for the refrigeration system performance improvement. Figure 1 shows a Mollier diagram of R134a accompanied with thermodynamic characteristics of a refrigeration system with and without a SLHX. The SLHX is a device where the capillary tube and the suction line tube are soldered together to form a lateral counter flow heat exchanger. In this paper, the effects of SLHX on the performance of refrigeration system are analyzed through the cycle simulation. The simulation is applied to a domestic refrigerator since it usually incorporates SLHX.

2. MODELS AND SIMULATION ALGORITHM

2.1 Compressor
The compressor performance was represented by the map-based model proposed by Fiscker and Rice (1980). The map-based compressor model uses empirical performance curves. These performance curves provide the refrigerant mass flow rate as functions of the condenser and the evaporator saturation temperatures. The mass flow rate is given by Eq. (1).

$$\dot{m}_{map} = b_1 T_e^2 + b_2 T_e + b_3 T_c^2 + b_4 T_c + b_5 T_e T_c + b_6 \tag{1}$$

Where, b, $\dot{m}$ and T represent the coefficient, mass flow rate, and temperature, respectively. The subscripts map, e, and c represent the map superheat conditions, evaporator, and condenser, respectively. The map-based model applies correction factors to the empirical curve fits to model the compressor at actual operating conditions. Dabri and Rice (1981) suggested the following equation:

$$\dot{m} = \left(0.75 \frac{v_{suc,map}}{v_{suc}} + 025\right)\dot{m}_{map} \tag{2}$$

Where, v represents specific volume. In this simulation program, the compression process is assumed to be isentropic. The refrigerant enthalpy at compressor discharge port is calculated based on entropy at compressor discharge and condenser pressure.

2.2 Condenser
The heat transfer rate, Q, is given by Eq. (3).

$$Q = UA(T_{ref} - T_{air}) \tag{3}$$

Where, U and A represent the overall heat transfer coefficient and heat transfer area. The subscripts ref and air represent the refrigerant and air, respectively. The overall heat conductance, UA is given by Eq. (4).

$$\frac{1}{UA} = \frac{1}{h_i A_i} + \frac{\ln(D_o/D_i)}{2\pi k_w L} + \frac{1}{h_o(A_o - A_{fin}(1-\eta))} \tag{4}$$

Where, h, D, k, L and η represent the heat transfer coefficient, tube diameter, tube thermal conductivity, tube length and fin efficiency. The subscripts o, i, w, and fin represent tube outside, inside, tube wall, and fin, respectively. The air-side heat transfer coefficient is calculated by the correlation suggested by Hilpert (1933).

$$\overline{Nu}_{D_o} = \frac{\overline{h}D_o}{k} = 0.193 Re_{D_o}^{0.618} Pr^{1/3} \tag{5}$$

The correlation of the heat transfer coefficient of refrigerant differs as a state of refrigerant. As single phase flow of refrigerant, the heat transfer coefficient is used the correlation suggested by Gneilinski (1976). The correlation is given by Eq. (7).

$$Nu = \frac{(f/2)(Re-1000)Pr}{1+12.7(f/2)^{1/2}(Pr^{2/3}-1)} \quad \text{where, } f = (1.58\ln Re - 3.28)^{-2} \tag{6}$$

The heat transfer in forced convection condensation is calculated using the correlation suggested by Cavalini and Zecchin (1974), which is as follows:

$$h_{tp} = 0.05 Re_{eq}^{0.8} Pr_{ref}^{0.33} \frac{k_{ref}}{D_i} \tag{7}$$

Where, the subscripts tp and eq stand for two-phase flow and equivalent, respectively. Re_{eq} is defined as Eq. (8).

$$Re_{eq} = Re_v\left(\frac{\mu_v}{\mu_l}\right)\left(\frac{\rho_l}{\rho_v}\right)^{0.55} + Re_l \tag{8}$$

Where, μ and ρ represent the density and kinetic viscosity. The subscripts v and l represent vapor phase and liquid phase of refrigerant. In Eq. (8), Re_v and Re_l are defined as follows:

$$Re_v = \frac{GxD}{\mu_v} \tag{9}$$

$$Re_l = \frac{G(1-x)D}{\mu_l} \tag{10}$$

Where, G and x represent mass flux ($4\dot{m}/\pi D^2$) and quality, respectively. The Pressure drop in refrigerant flow is calculated from the Fanning equation as follows:

$$\Delta P = \frac{2fG^2L}{D\rho} \quad . \tag{11}$$

Churchill's model (1977) is used for pressure drop calculation of single phase refrigerant flow. Where, f_{sp} is the single-phase friction factor and is given by Eq. (12).

$$f_{sp} = 8\left[(\frac{8}{Re_{sp}})^{12} + \frac{1}{(A+B)^{1.5}}\right]^{1/12} \tag{12}$$

Re_{sp}, A, and B is defined as follows:

$$Re_{sp} = \frac{GD}{\mu} \quad , \tag{13}$$

$$A = \left\{2.457\ln\left[\frac{1}{(7/Re_{sp})^{0.9} + 0.27/D_i}\right]\right\}^{16} \quad , \tag{14}$$

$$B = \left(\frac{37530}{Re_{sp}}\right)^{16} \quad . \tag{15}$$

For two-phase flow pressure drop, the two-phase friction factor, f_{tp} is given by Eq. (16).

$$f_{tp} = \varphi_{lo}^2 f_{sp}\left(\frac{v_{sp}}{v_{tp}}\right) \tag{16}$$

The two-phase multiplier, φ_{lo}^2 in Eq. (16) was suggested by Lin et al (1991) as follows:

$$\varphi_{lo}^2 = \frac{\left[\left(\frac{8}{Re_{tp}}\right)^{12} + \frac{1}{(A_{tp} + B_{tp})^{1.5}}\right]^{1/12}}{\left[\left(\frac{8}{Re_{sp}}\right)^{12} + \frac{1}{(A_{sp} + B_{sp})^{1.5}}\right]}\left[1 + x\left(\frac{v_v}{v_l} - 1\right)\right] \quad . \tag{17}$$

Where, Re_{tp} is defined as follows:

$$Re_{tp} = \frac{GD}{\mu_{tp}} \quad \text{where,} \quad \frac{1}{\mu_{tp}} = \frac{x}{\mu_v} + \frac{1-x}{\mu_l} \tag{18}$$

2.3 Evaporator

The overall heat conductance, UA is equal to Eq. (4). In the evaporator, the convective boiling heat transfer coefficient is calculated based on Chen (1966)'s correlation, in which convective boiling effect and nuclear boiling effect are superposed as follows: .

$$h_{tp} = h_{cb} + h_{nb} = h_{lo}F_o + h_pS \quad . \tag{19}$$

Where, F and S represent boiling enhancement factor and suppression factor. The subscripts lo and P represent liquid only and pool boiling. The parameter F_o is defined by Eq. (20)

$$F_o = F(1-x) \quad \text{where} \begin{cases} \text{For } 1/X_{tt} \le 0.1, F = 1 \\ \text{For } 1/X_{tt} > 0.1, F = 2.35(0.213 + 1/X_{tt})^{0.736} \end{cases} \tag{20}$$

Where, The Martinelli parameter X_{tt} is defined by Eq. (21).

$$\frac{1}{X_{tt}} = \frac{x}{(1-x)^{0.9}}\left(\frac{\rho_l}{\upsilon_v}\right)^{0.5}\left(\frac{\mu_v}{\mu_l}\right)^{0.1}.$$ (21)

The liquid-phase heat transfer coefficient, h_{lo} is estimated by Dittus-Boelter's correlation.

$$h_{lo} = 0.023Re^{0.8}Pr^{0.4}\frac{k_l}{D}$$ (22)

The suppression factor, S, is defined by Eq. (23).

$$S = \left[\Delta T_{sup}/\Delta T_{sat}\right]^{0.99}$$ (23)

Where, the subscripts sup and sat represent mean superheat and saturation. Forster and Zuber (1955)'s correlation is used for the pool boiling heat transfer coefficient, h_p.

$$h_p = 0.00122\left[\frac{k_f^{0.79}c_{pf}^{0.45}\rho_f^{0.49}}{\sigma^{0.5}\mu_f^{0.29}i_{fg}^{0.24}\rho_g^{0.24}}\right]\Delta T_{sup}^{0.24}\Delta P_{sup}^{0.75}$$ (24)

Where, c_p and σ represent specific heat and surface tension. Single phase heat transfer coefficient, single phase friction factor correlations and two-phase friction factor correlations used for evaporator calculation are the same as those used for the condenser calculation.

2.4 Capillary tube and Suction line heat exchanger

Figure 2 shows the cross-section of a welded SLHX. Heat transfer will take place between the refrigerants flowing inside a capillary tube and a suction line pipe as the refrigerant temperature at capillary tube is higher than that at the suction line pipe. The heat transfer rate of the SLHX is given by Eq (25).

$$Q_{SLHX} = UA(T_{capi} - T_{suc})$$ (25)

Where, the subscripts capi and suc represent capillary tube and suction line. The overall heat conductance (UA) of the SLHX is given as follows:

$$\frac{1}{UA_{SLHX}} = \frac{1}{h_{capi}A_{capi}} + \frac{\ln(D_{capi,o}/D_{capi,i})}{2\pi k_{capi,w}dz} + \frac{\delta}{k_{solder}wdz} + \frac{\ln(D_{suc,o}/D_{suc,i})}{2\pi k_{suc,w}L} + \frac{1}{h_{suc}A_{suc}}$$ (26)

Where, k_{solder}, δ and w represent thermal conductivity, thickness, and width of the welding. The convective heat transfer coefficients at the inner wall of the suction line pipe and liquid-phase region of capillary tube are evaluated using Gneilinski's model, Eq. (6). For two-phase region of SLHX, the most of thermal resistance lies on the suction line side so that the capillary-side convective heat transfer coefficient is assumed to be infinite. The validity of this assumption has been confirmed by Mezavila et al (1996). Eq. (12) and (16) are used to estimate the frictional head loss in capillary tube and suction line pipe.

2.5 Cycle Simulation Algorithm

Figure 3 shows a schematic for the refrigeration cycle with SLHX that is simulated in the present work. Mathematical model of each component described in the previous sections are used to build a set of equations. The equation set is calculated using Newton-Raphson method.
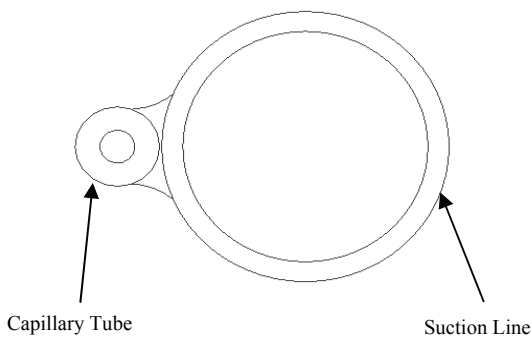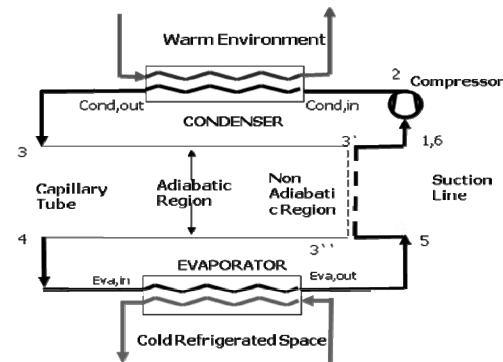

Figure 2: Cross section of a SLHX

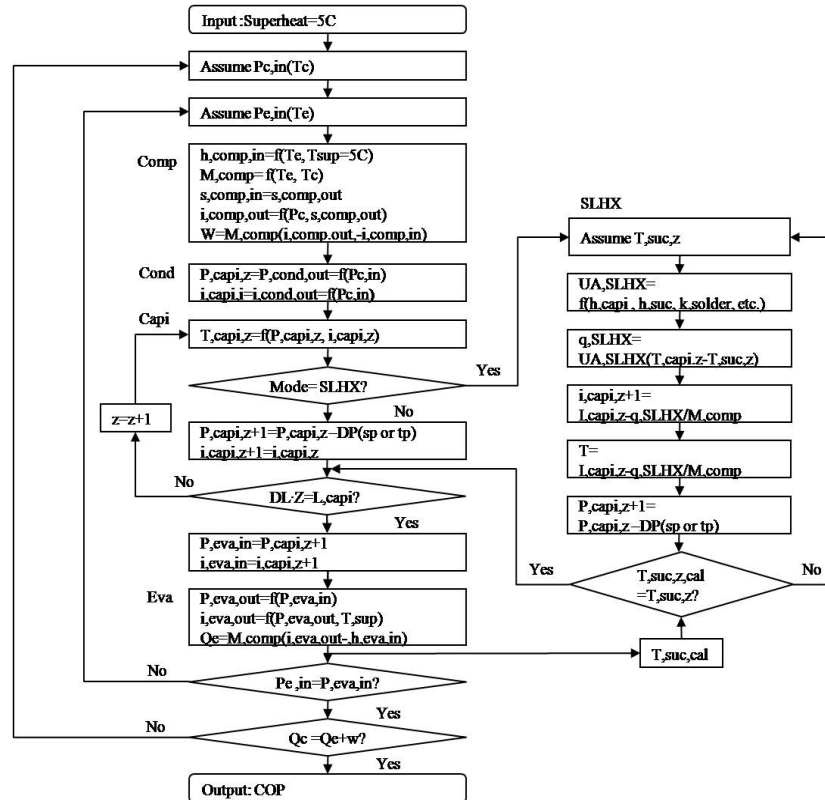Figure 3: Schematic for the refrigeration cycle system

Figure 4: Flow chart of simulation program

Algorithm of the present cycle simulation is shown in Figure 4. Cycle simulation input includes evaporator and condenser specifications, air flow rates at condenser and evaporator, ambient and cabinet temperature, evaporator outlet superheat (or refrigerant charge of system). The pipes connecting components are not considered except suction line pipe which is located between evaporator and compressor.

3. CYCLE SIMULATION RESULTS

A domestic refrigerator without SLHX was selected as a reference refrigeration cycle for this study. Specifications for this system are summarized in Table.1. All geometric and operating conditions are fixed for comparative analyses except SLHX geometry. The length and the location of the SLHX were changed and the results were compared with each other in terms of refrigeration effect, compressor work, coefficient of performance (COP), etc. The COP of a refrigeration cycle is defined as follows:

$$COP = \frac{\text{Cooling capacity}}{\text{Compressor work}} = \frac{i_{eva,out} - i_{eva,in}}{i_{comp,out} - i_{comp,in}} \qquad (27)$$

Where, the subscripts eva and comp represent the evaporator and the compressor.

Table 1: Simulation condition of the refrigeration cycle

|			
Refrigerant	R134a	Capillary Tube Inner Diameter	0.0006 (m)
Superheating at Evaporator Out	5 ('C)	Capillary Tube Outer Diameter	0.002 (m)
Ambient Air Temperature	25('C)	Suction Line Inner Diameter	0.006 (m)
Refrigeration Room Air Temp	-10('C)	Suction Line Outer Diameter	0.009 (m)
Condenser length	18m	Condenser Inner Diameter	0.004 (m)
Evaporator length	7.5m	Condenser Outer Diameter	0.0047 (m)
Capillary Tube Length	2.5m	Evaporator Inner Diameter	0.0072 (m)
Suction Line Length	2.5m	Evaporator Outer Diameter	0.008 (m)
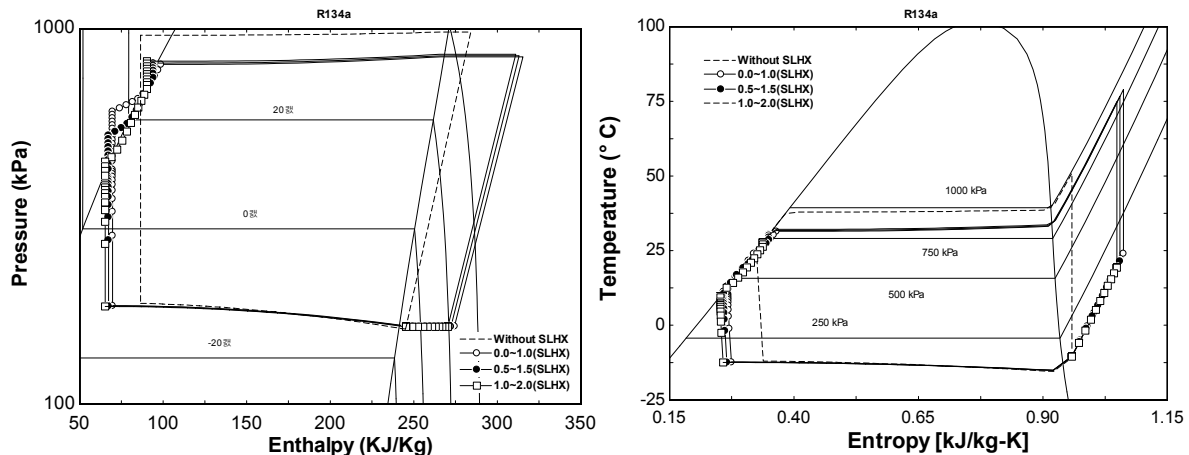
Figure 5: Log(P)-i diagram and T-s diagram for R134a cycle with and without SLHX

Cycle performance simulations have been performed with various lengths of soldered region and soldering location. Figure 5 shows thermodynamic properties of refrigeration cycles simulated in Mollier diagram as well as T-s diagram. The length of soldered region is set constant at 1.0m while the location changes from the entrance to exit of capillary tube. Refrigeration cycle with no heat exchange between capillary tube and suction-line tube is also compared in the plots as a reference case. Also important values for these cycles are summarized in Table 2. Table 2 and Figure 5 show the performance of R-134a refrigeration cycle is enhanced by the existence of SLHX and also influenced by the location of the soldered region. This change in COP is caused by the relatively larger increase in refrigeration effect compared with less increase in compression work.

Further simulation results are compared in Figure 6~9. Vertical axis indicates the COP ratio in percent compared with a cycle without the SLHX. Horizontal axis indicates the location along a capillary tube of which length is 2.5m. Each horizontal line in these plots represents the location of soldering region between capillary tube and suction line pipe. Figure 6 shows the COP change with an increase in the SLHX region from the capillary entrance.

This plot shows the COP decreases with an increase in SLHX length when it is short (A to B). However, the COP starts to increase with a further increase in SLHX length (B to C). An opposite trend is observed when the SLHX length is increased from the capillary tube exit as can be seen in Figure 7. Figure 8 shows the COP increases with an increase in SLHX length when its center is located in the middle of the capillary tube. Figure 9 shows the influence of soldering location. For this comparison, the lengths of soldering regions of all cases are set to be 1 meter long. This plot shows the maximum COP is obtained when the soldering region is located near the capillary tube exit. However, COP decreases at the very exit.

Table 2: Simulation condition of the refrigeration cycle

SLHX Region (m)	No HX	0~1	0.5~1.5	1~2
Condenser inlet pressure (KPa)	979.5	842	847.2	854.3
Evaporator outlet pressure (KPa)	158.5	161.7	161.2	160.8
Condensing temperature ('C)	38.6	33.12	33.34	33.63
Evaporation temperature ('C)	-15.84	-15.35	-15.42	-15.49
Condenser outlet subcooling ('C)	12.89	Two Phase	1.38	4.45
Evaporator outlet superheating ('C)*	5	5	5	5
Mass Flow Rate (g/s)	0.6243	0.5699	0.5723	0.5745
Refrigerant Charge (g)	151.2	35.29	40.97	49.96
Refrigeration Effect (KJ/Kg)	158.7	175.8	178.1	180.1
Heat Transfer in SLHX (KJ/Kg)	0	29	26.87	25.02
Heat transfer rate to ambient(KW)	0.1234	0.1070	0.1100	0.1125
Cooling Capacity (KW)	0.09908	0.1002	0.102	0.1035
Compression Work (KW)	0.02432	0.02332	0.02332	0.02337
COP	4.074	4.296	4.371	4.428

* Only constraint for simulations. Constant refrigerant charge may replace this constraint for simulations.
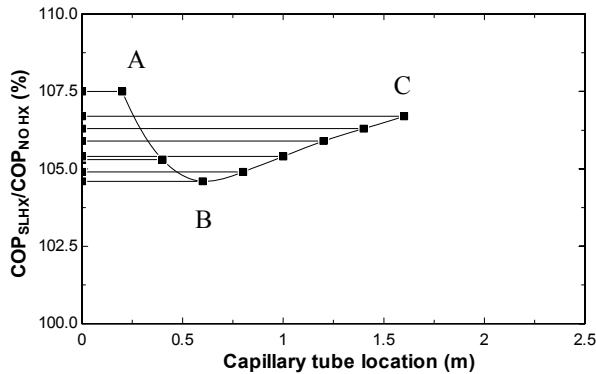
Figure 6: COP change in accordance with SLHX length variation at the capillary entrance
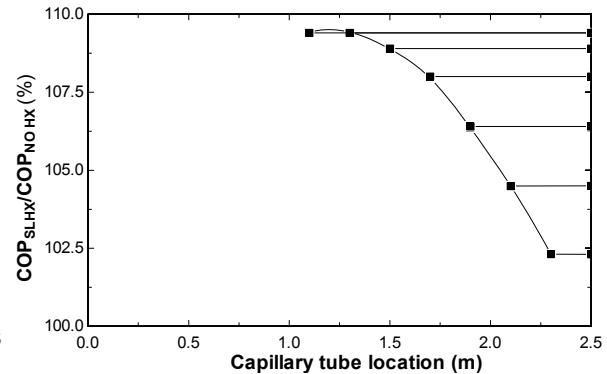

Figure 7: COP change in accordance with SLHX length variation at the capillary exit
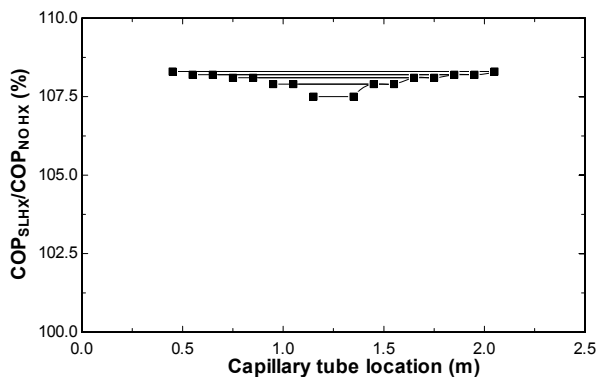

Figure 8: COP change in accordance with SLHX length variation at the capillary middle
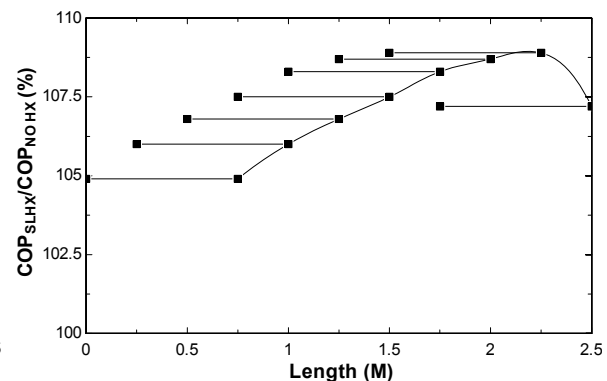

Figure 9: COP change in accordance with SLHX location

Through the all cases simulated, the SLHX enhances COP of refrigeration cycle by up to 109% compared to the cycle without SLHX. Also these plots show that the influence of SLHX onto the refrigeration cycle performance is not monotonous. It is observed that COP increases with an increase in SLHX length in some range but turns to decrease over a certain range. The influence of SLHX location also shows a similar trend. In other words, there is an optimal soldering location and length for SLHX.

4. CONCLUDING REMARKS

The performances of refrigeration cycle with various SLHX specifications were simulated in order to study the influence of SLHX on small size refrigeration system. Simulations were performed with the same design specifications only except SLHX itself. The length and the location of soldering region between capillary tube and suction-line tube were changed and the performance of refrigeration cycle was compared in terms of condenser pressure, evaporator pressure, refrigeration effect, compressor work, and COP. In the present study, a constraint of constant evaporator superheat was applied to all simulations. Based on the simulation results, following conclusions may be drawn:

(1) Adoption of SLHX has beneficial effects to the R-134a small refrigeration cycle. The COP was increased by up to 9% compared with simple refrigeration cycle.

(2) The influences of the length and location of soldering region for SLHX are not monotonous so that optimization is required for practical design of small refrigeration system.

NOMENCLATURE

A	cross sectional area	(m^2)	**Greeks**			
c	specific heat	(Jkg/K)	ε	wall roughness	(mm)
D	diameter	(m)	δ	solder joint thickness	(m)
f	friction factor		ρ	density	(kg/m^3)
G	mass flux	(kg/m^{2}s)	σ	Surface tension	(N/m)
g	gravity acceleration	(m/s)	μ	viscosity	(Ns/m^2)
i	specific enthalpy	(kj/kg)			
h	heat transfer coefficient	(W/m^{2}k)	**Subscripts**		
k	conductivity	(W/mK)	cappi	capillary tube
L	length	(m)	c	condenser
m	mass flow rate	(kg/s)	e	evaporator
Nu	Nusselt number		i	inside
Pr	Prandtl number		in	inlet
P	pressure	(KPa)	HX	heat exchanger
Q	Heat transfer rate	(kW)	l	liquid
Re	Reynolds number		o	outside
T	temperature	(K)	out	outlet
U	overall heat transfer coefficient	(W/m^{2}k)	s	suction line
v	specific volume	(m^3/kg)	sp	single-phase
Work	specific work	(kW)	sub	subcooling
w	width of solder joint	(m)	sup	superheating
x	vapor quality		tp	two-phase
x_{tt}	martinelli Parameter		v	vapor

REFERENCE

Cavallini, A. and Zecchin, R., 1974, A dimensionless correlation for heat transfer in forced convection condensation, Proc. 5th Heat Transfer Conf, Tokyo, Japan, September, 3~7: p. 309-313.

Chen, J. C., 1966, A correlation for boiling heat transfer to saturated fluids in convective flow, Ind. Eng. Chem. Process Des. Dev., Vol. 5: p. 322-329.

Churchill, S. W., 1977, Friction equation spans all fluid flow regimes, Chemical Engineering, Vol. 84, p. 91-92

Dabiri, A. E. and Rice, C. K., 1981, A compressor simulation method with corrections for the level of suction gas superheat, ASHRAE Trans., Vol. 87.

Domanski, P. A., 1982, Computer modeling and prediction of performance of an air source heat pump with a capillary tube, Ph.D. Dissertation, The Catholic Univ. of America.

Fischer, S. K. and Rice, C. K., 1980, The Ork Ridge heat pump models: 1 A steady-state computer design model for air to air heat pumps, ORNL/CON-80/R1, Energy Division, Ork Ridge National Lab.

Forster, H. K. and Zuber, N. 1955, Dynamics of vapor bubbles and boiling heat transfer, AICHE journal, Vol. 1, No. 4: p. 531-535.

Gneilinski, V., 1976, New equation for heat and mass transfer in turbulent pipe and channel flow, International Journal of Chemical Engineering, Vol. 16: p. 359~368.

Hilpert, R., 1933, *Forsch. Geb. Ingenieurwes.*, Vol. 4, 215p.

Hitler, C. C. and Glicksman, L. R., 1976, Improving heat pump performance via compressor capacity control-Analysis and test, MIT EL 76-001, Energy Laboratory, Massachusetts Institute of Technology, Vol. I and II.

Lin, S. et al., 1991, Local frictional pressure drop during vaporization of R-12 through capillary tubes, International Journal of Multiphase Flow, Vol. 17, No. 1: p. 95-102.

Mezavila, M. M., Melo, C., 1996, CAPHEAT: a homogeneous model to simulate refrigerant flow through non-adiabatic capillary tubes, International Refrigeration Conference at Purdue: p. 95-100.